Int j simul model 23 (2024) 4, 656-667
Original scientific paper

CUTTING VIBRATION RESPONSE OF A SHIELD-TYPE TUNNELLING ROBOT SYSTEM

Ma, H. W.[*,**]; Xue, L. M.[*,**,#] & Wang, C. W.[*,**]

[*] School of Mechanical Engineering, Xi'an University of Science and Technology, Xi'an 710054, China

[**] Shaanxi Provincial Key Laboratory of Intelligent Testing and Control of Mine Mechanical and Electrical Equipment, Xi'an University of Science and Technology, Xi'an 710054, China

E-Mail: xuelm@xust.edu.cn ([#] Corresponding author)

Abstract

To improve the tunnelling-cutting efficiency, enhance the overturning stability of the tunnelling-cutting system, a shield-type tunnelling robot system was proposed, a load model of the cutting drum was established, and the cutting and tractive resistance were obtained. Force and overturning stability models were constructed. The stability coefficient was put forward, a multirigid-body dynamic model was built, and a model of the conditions for maintaining stability and a model of the vibration displacement response law were established. A simulation experiment and an underground on-site coal and rock section cutting test were performed, and the overall system stability and the vibration displacement response of each component were compared to verify the correctness of this study. Results prove that the proposed stability coefficient can significantly improve the overall stability by giving the shield the force to adapt to the cutting load. The transverse and longitudinal vibration displacement responses of the cutting drum to upper and lower shields decrease successively. The maximum transverse and longitudinal displacements are 9.27 and 11.68 mm, respectively.

(Received in September 2024, accepted in October 2024. This paper was with the authors 1 week for 1 revision.)

Key Words: Shield Type, Cutting Robot, Multirigid-Body Model, Stability, Vibration Response

1. INTRODUCTION

Given the harsh and complex underground driving environment in coal mines, tunnelling-cutting equipment vibrates easily in the tunnelling process of roadways, aggravating instability, causing a decline in cutting efficiency, and even leading to safety accidents of personnel and equipment [1, 2]. Moreover, the intelligent development of coal mining has been restricted by such long-term problems as fast coal mining but slow tunnelling and fast tunnelling but slow supporting. Coal roadheaders, which can considerably improve the tunnelling-cutting efficiency and safety of coal mine roadways, have been widely applied in the tunnelling of some large-scale coal mine roadways. With the development of the coal industry, the technical level of a fully mechanized coal mining face and the equipment level have been continuously improved, and intelligent development has been preliminarily achieved. As coal mining speed and efficiency are further improved, elevated requirements for coal mine roadway tunnelling have been proposed, and the contradiction of "fast mining and slow tunnelling" becomes increasingly prominent. Studying tunnelling robot systems and realizing tunnelling-support and tunnelling-anchoring synchronous operations have become a domestic and foreign research hotspot regarding the tunnelling of coal mine roadways.

Chinese and foreign scholars have extensively analysed tunnelling-support parallel operations. Multiple models of tunnelling-anchoring all-in-one machines have been developed to realize an integrated tunnelling process and a parallel operation of tunnelling for coal cutting and anchor bolt support. For instance, German DHMS and Japanese Mitsui Miike, which are representative companies, have developed roadheaders based on cantilever roadheaders, realizing parallel operations of tunnelling cutting and temporary support [3]. U.S. Joy CM series continuous coal winning machine and other rapid tunnelling equipment for continuous coal

mining are used for double- or multi-roadway tunnelling, and MB670 from Sandvik Company of Sweden and 12ED30 tunnelling-anchoring integrated unit from Joy Company of the U.S. with improved tunnelling efficiency have been widely utilized in coal mine roadway tunnelling at home and abroad [4]. The research on domestic tunnelling equipment started late, and the current research direction focuses on rapid tunnelling systems, which have been successfully developed and initially applied, such as the rapid tunnelling system of China Railway Construction Heavy Industry Corporation Limited and the rapid tunnelling system of Taiyuan Research Institute of China Coal Technology & Engineering Group. The research and application of all-in-one machines for excavating and anchoring and rapid tunnelling systems have improved the tunnelling speed of coal mine roadways and reduced the number of workers in the tunnelling face. However, the cross-section cutting heads of these tunnelling systems are all open structures, and the stability of the entire machine mainly depends on the gravity of the machine body. Some problems remain, e.g., the entire machine of the tunnelling-cutting system jumps, the vibration displacement response of the system components is considerably large, the requirements for the tunnelling-cutting conditions of roadway coal and rock are high, and the adaptability is poor. Ensuring the stability of the whole system, mastering the vibration response law of each part of the tunnelling equipment, and reducing the vibration displacement are theoretically and practically significant to improve the adaptability of the rapid tunnelling system and realize stable and efficient tunnelling cutting.

2. STATE OF THE ART

Given the complexity of coal occurrence conditions, obtaining the cutting load is always difficult, which brings challenges to the research and development of tunnelling equipment. Foreign research in this field started earlier. the influence of cutting pick and cutting head on the cutting process and analysed the change in cutting force were analysed by simulation [5-8]. The load of the cutting head through a mathematical or experimental method were obtained [9-11]. Aiming at the complicated roadheader-based coal and rock cutting process and taking the cutting head of a longitudinal roadheader as the study object. A tunnelling model of coal and rock cutting in accordance was established with the cutting parameters determined by experiments, a simulation was performed, and the cutting load and its variation law was analysed [12]. The relationship between cutting state parameters and cutting load was evaluated by mathematics and the finite element method [13]. The load of the cutting head of a longitudinal roadheader, the dynamics of the cutting head and the stress of the cutting condition were analysed, and the formulas for cutting resistance and tractive resistance of the cutting head were deduced [14]. A solid model of a roadheader was established with three-dimensional software and a load simulation of the cutting head was performed via Adams [15]. The abovementioned studies mainly focused on the load analysis of cutting picks or the simulation of the cutting head of longitudinal roadheaders to obtain the cutting load, with single conditions, partially large deviations, or poor adaptability to the cutting load of full-section transverse cutting drums.

In the aspect of system overturning stability, the static stability of a certain type of tunnelling-anchoring integrated machine was analysed and it was concluded that overturning and sliding would not occur within the specified slope range [16]. The stability equation of a roadheader was established by analysing the torque and force borne by the roadheader. Based on the analysis of an example, the critical stable state along the vertical axis was the critical stable state of the roadheader [17]. The mathematical expression of the stability condition under the working condition of transverse cutting of a cantilever roadheader was given through mechanical calculation and derivation [18]. The performance indexes of a semi-coal and rock roadheader was analysed and it was stated that working stability is an important index for

evaluating the performance of the entire machine, which directly affects the cutting performance and working reliability of the roadheader. The scholar also analysed the stress situation of the semi-coal and rock roadheader in the static state of upward or downward slope, downward travel along the maximum downward slope, upward or downward cutting, and longitudinal drilling cutting [19]. The longitudinal stability condition of an EBZ260 roadheader was put forward under the limit working condition [20]. The no-load static stability of an EBH315 roadheader and its static stability under cutting conditions based on the static stability conditions of a cantilever roadheader were analysed [21]. The above studies on the stability of roadheaders aimed at the system overturning, sliding, or rotation generated within a specific slope range and explored the stability within conditions based on the gravity of roadheaders, accompanied with the fact that open structures keep stable by relying on gravity.

In the aspect of cutting vibration response, scholars established the dynamic model of a longitudinal roadheader through simulation software and determined its related parameters [22], constructed a vibration transmission path model by path analysis and analysed the source of vibration [23]. Physical models of the cutting part and swing mechanism of a longitudinal roadheader was established, the models were simulated and analysed by simulation, and the vibration and stability of each component were predicted [24, 25]. The dynamic equation of a longitudinal roadheader were established, the cutting arm of the longitudinal roadheader was simulated and analysed in Adams [26]. Cutting dynamic and cutting vibration models of a longitudinal roadheader were established and the vibration displacement was analysed by simulation [27]. The aforementioned studies assessed the vibration of each component of open-type roadheaders by simulation, while shield-type structures with a shield supporting the roof and floor remain to be deeply explored.

Such related achievements in China and abroad mainly concentrated on the cutting load, overturning stability on different roadway slopes, and cutting vibration response of longitudinal roadheaders. Full-section transverse tunnelling-cutting equipment has been scarcely analysed. Meanwhile, the stability of shield-type tunnelling cutting and supporting integrated equipment has been investigated minimally, not to mention the cutting vibration displacement response and transfer laws. With a shield-type tunnelling robot as the study object, a load model for the cutting drum was established, and the relational models of cutting parameters with the cutting resistance and tractive resistance borne were acquired. Mechanical and multirigid-body dynamic models were built, laying a foundation for the research on system stability and vibration displacement response. The stability coefficient for the tunnelling robot system was proposed, and the conditions to keep stable were explored. Simulation and field tests were designed, the correctness of the conditions for keeping the system stable was verified, and whether the vibration displacement response of each system component met the cutting requirements of the roadway section was determined.

The remainder of this paper is organized as follows: In Section 3, based on the structural principle and characteristics of the shield-type tunnelling robot, a cutting drum load model, system stability and multirigid-body dynamic models, and a virtual prototype of the shield-type cutting robot were established, which provided a basis for the simulation experiment. In Section 4, the system stability and vibration displacement response were subjected to a simulation analysis, and a field test platform was designed and erected for test and application. In Section 5, conclusions were drawn.

3. METHODOLOGY

3.1 Shield-type tunnelling robot model

To realize the intellectualization of rapid tunnelling of large-section semi-coal and rock roadways in complex geological conditions and improve the cutting efficiency and unmanned

(less manned) goal, a team led by Ma [28] designed and developed a rapid tunnelling robot system for coal mine roadways, as shown in Fig. 1. The system is mainly composed of cutting robot, temporary support robot (shield) I & II, drilling and anchoring robot, electrohydraulic control platform, ventilation and dust removal system, and transportation system. Among them, the cutting robot is the vanguard of the whole rapid tunnelling system. In this study, the shield-type cutting robots in the system were taken as the study objects, which were composed of temporary support robot (shield) I (including upper and lower shields) and a cutting robot (sliding table, cutting arm, cutting drum, shovel plate, etc.) as shown in Fig. 2. The cutting robot was integrated with the lower shield through its sliding table. The cutting operation was completed by the upward and downward swinging of the cutting arm, the horizontal movement of the sliding table, and the rotation of the cutting drum. Temporary support robot (shield) I supported the roof and floor of the roadway through the upper and lower shields and the support cylinder, exerting the functions of temporary supporting and cutting robot stabilization. Temporary support robots (shield) I and II cooperated with each other to drive the tunnelling system to move forward and backward.

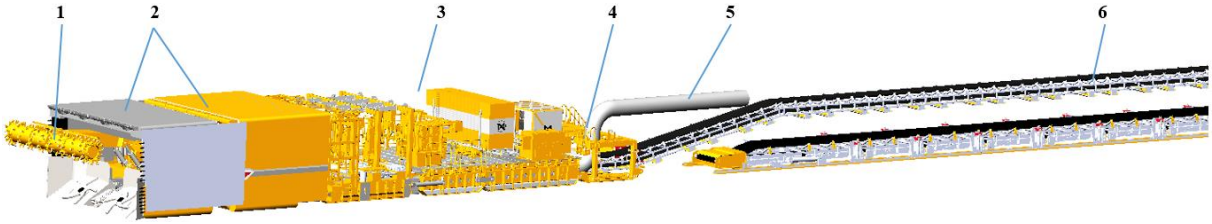

Figure 1: Rapid tunnelling robot system for coal mine roadways; 1 – Cutting robot, 2 – Temporary support robots (shield) I and II, 3 – Drilling–anchoring robot, 4 – Electrohydraulic control platform, 5 – Ventilation and dust removal system, 6 – Transportation system.

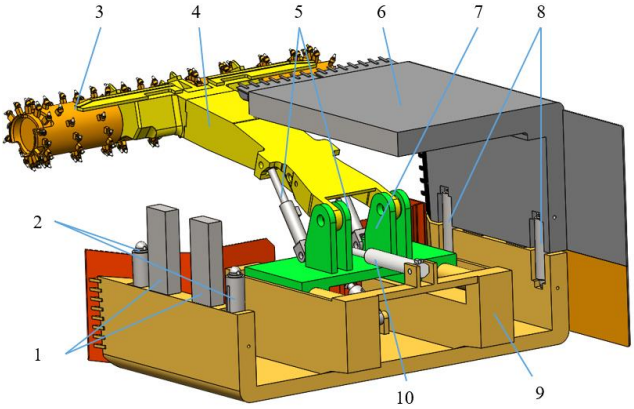

Figure 2: Shield-type cutting robot; 1 – Guide post, 2 – Lifting support cylinder, 3 – Cutting drum, 4 – Cutting arm, 5 – Cutting arm oil cylinder, 6 – Upper shield, 7 – Sliding table, 9 – Lower shield, 10 – Sliding table pushing cylinder.

3.2 Cutting drum load model

The coal and rock section cutting operation of the tunnelling robot started from each pick on the cutting drum. The force borne by the pick on the cutting drum should be analysed. Because of the complex coal and rock cutting environment, the cutting drum was subjected to cutting resistance, cross-section friction, and other different effects, presenting irregularity and randomness. Therefore, cross-section cutting should be properly simplified. The force borne by each cutting pick of the drum during the cutting process could be converted into the axial cutting resistance Y_i of the cutting drum and the tractive resistance tangential to the section, as shown in Fig. 3.

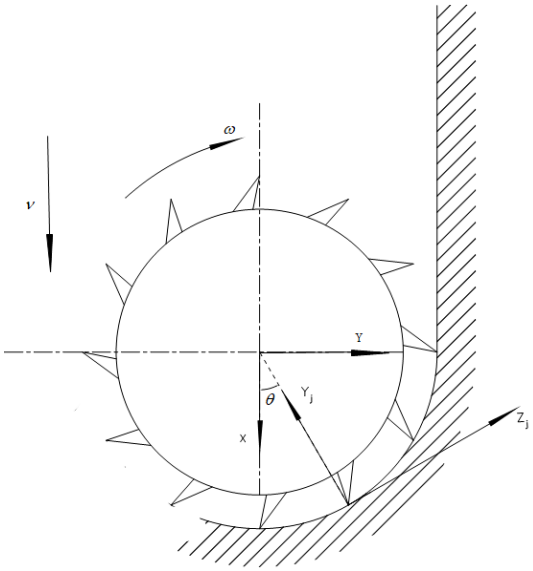

Figure 3: Single cutting force.

Under general circumstances, cutting picks will be worn. After being worn blunt, the cutting picks contact with the cut section into one plane. In this case, the cutting resistance Z_{ij} borne by the i^{th} cutting pick on the j^{th} transversal cutting line is [14, 29]:

$$Z_{ij} = P_k\,[k_r\,k_f\,k_f'\,k_d\,k_y'\,(0.25 + 1.8\,h_{ij}\,\sin\theta_{ij} \times t_i) + 0.1S_i] \tag{1}$$

The cutting tractive resistance is solved as follows:

$$Y_{ij} = \frac{2.5\,Z_{ij}(0.15 + 0.0056\,P_K)}{\sqrt[4]{10\,h_{max}\sin q}} \tag{2}$$

where, Z_{ij} – Cutting resistance; Y_{ij} – Tractive resistance; P_k – Coal-rock contact strength coefficient; k_γ – Type coefficient of cutting picks; k_φ – Shape coefficient of the cutting drum; k'_φ – Shape coefficient of the cutting drum; k_d – Diameter coefficient of the cutting drum; k'_y – Influence coefficient of the cutting angle; θ_{ij} – Cutting angle of cutting picks; S_{ij} – Projection of cutting picks' wear surface on the section.

The cutting resistance and tractive resistance of all cutting picks on the j^{th} transversal cutting line were projected in the cutting robot coordinate system, and the projections of the forces borne by all cutting picks were summed. On this basis, the cutting resistance Z_j and tractive resistance Y_j borne on the j^{th} transversal cutting line of the cutting drum can be solved as follows:

$$\begin{cases} Z_j = \sum_{i=1}^{n}(-Y_{ij}\cos\theta_{ij} - Z_{ij}\sin\theta_{ij}) \\ Y_j = \sum_{i=1}^{n}(-Y_{ij}\sin\theta_{ij} + Z_{ij}\cos\theta_{ij}) \end{cases} \tag{3}$$

The cutting resistance and tractive resistance on all transversal cutting lines were summed to obtain the cutting resistance and tractive resistance counter-accepted by the cutting drum, as displayed in the following formula:

$$\begin{cases} R_z = \sum_{j=1}^{m} Z_j \\ R_y = \sum_{j=1}^{m} Y_j \end{cases} \tag{4}$$

3.3 Mechanical model of the cutting robot

The temporary support robot supported the roadway roof and floor when the shield-type tunnelling robot cut the coal and rock. The forces borne by the whole system included system gravity, floor support force F_{y1}, roof pressure F_{y2}, roof friction f_2, floor friction f_1, sectional cutting resistance R_z and tractive resistance R_y, i.e., the forces decomposed by the cutting force into the axial and vertical directions of the roadway, and the internal acting force of the shield-type cutting robot, including the interaction force between each oil cylinder and connection point, as shown in Fig. 4. For keeping the system stable during cutting and preventing the system from bouncing around axis O because of the massive cutting force to avoid affecting the system safety and stability and impeding sectional cutting, the force and moment of the system should be balanced.

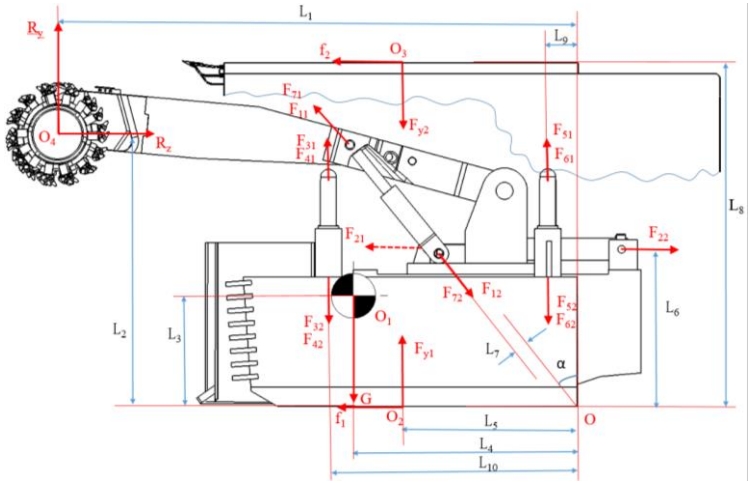

Figure 4: Cutting mechanical analysis of the shield-type cutting robot.

$$\begin{cases} \sum M = F_i \times L_i = 0 \\ \sum F_y = 0 \\ \sum F_z = 0 \end{cases} \tag{5}$$

For ensuring a stable and continuous cutting process and preventing tilting around axis O, the stabilizing moment M_s should be greater than the moment of cutting resistance M_o, i.e., the following cutting stability condition should be met [30]:

$$K = \frac{M_s}{M_o} \geq 1.1 \tag{6}$$

3.4 Multirigid-body dynamic model of the shield-type tunnelling robot

Through SolidWorks, each component of the shield-type tunnelling robot was drawn, and all components were assembled in accordance with the movement of roadway tunnelling cutting in the assembly environment. The attribute of each component was defined, and the constraint relationships were added. Motion examples were generated, and motion analysis was carried out to ensure that the three-dimensional model was free of interference and could meet the realization of the cutting motion relationship. Such parameters as cutting load, ground support force, roof pressure, cutting friction, and damping were added to the model, followed by re-examination and verification in the Adams environment, ensuring that the drive and constraint requirements of cutting were satisfied [31]. Then, a multirigid-body dynamic model of the shield-type tunnelling robot was constructed, as shown in Fig. 5.

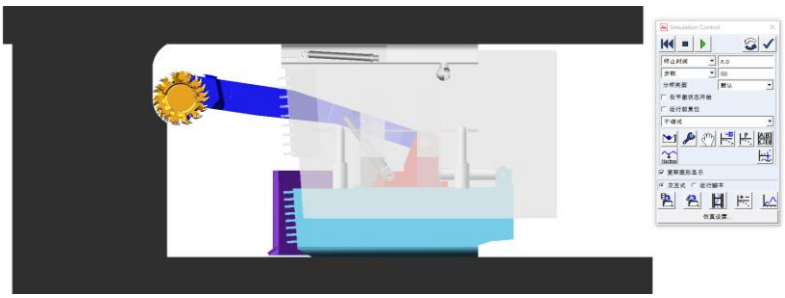

Figure 5: Multirigid-body dynamic model of the shield-type cutting robot.

4. RESULT ANALYSIS AND DISCUSSION

4.1 Simulation analysis

The relevant parameter of each part of the shield-type tunnelling robot is described as follows. The parameter specifications of the cutting drum included the mass of the cutting drum = 6235.349 kg, the mass of the cutting arm = 20031.67 kg, the mass of the sliding table = 11287.20 kg, the mass of the lower shield = 75416.49 kg, and the mass of the upper shield = 98669.34 kg. The stiffness coefficients of the cutting drum, cutting arm, sliding table, lower shield, and upper shield were 7.8 × 105, 6.8 × 105, 6.8 × 105, 3.7 × 103, and 3.7 × 103, respectively; their damping coefficients were 6.0 × 104, 3.6 × 104, 3.3 × 104, 3.4 × 104, and 3.4 × 104 N·s/m, respectively.

Based on the above, the load of the cutting drum and the pressure (tensile force) of the cutting arm's oil cylinder and sliding table's oil cylinder were solved, as shown in Fig. 7.

In Fig. 6, curve ① is the cutting resistance of the cutting drum, and curve ② represents the tractive resistance of the cutting drum. The load of the cutting drum showed periodically irregular changes, and the mean value and instantaneous peak value of the cutting resistance were 180 and 735 KN, respectively. Similarly, the load of the cutting drum presented periodically irregular changes, and the mean value and instantaneous peak value of the tractive resistance were 156 and 640 KN, respectively. The tractive resistance was 85 % of the cutting resistance. In Fig. 7, ① is the pressure (tensile force) curve of the sliding table's oil cylinder, and ② is the pressure (tensile force) curve of the cutting arm's oil cylinder. The pressure (tensile force) change of the two oil cylinders was roughly divided into two types: In Step 1, the oil cylinder of the sliding table moved backward, during which the mean value of the oil cylinder's output tensile force was great and gradually decreased, reaching the minimum value when the cutting arm moved to the horizontal position. In Step 2, the sliding table moved forward, and the thrust of the oil cylinder gradually increased. Meanwhile, the swing cylinder force of the cutting arm continued to decline, and the force gradually grew in the final stage.

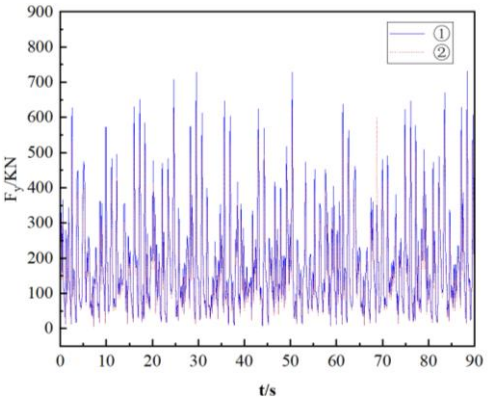

Figure 6: Load of the cutting drum.

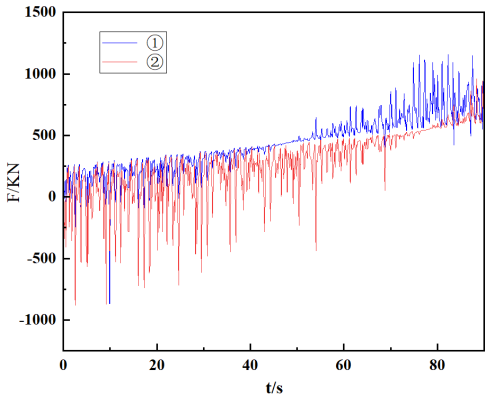

Figure 7: Pressure of the cutting arm's oil cylinder.

Bouncing stability of the cutting robot: In case of no interaction force between the upper shield of temporary support robot I and the roadway roof, i.e., $F_{y2} = 0$, Fig. 8 is obtained in accordance with the change and stability conditions for the cutting force. Therein, ① represents the stability coefficient, and ② denotes the instable interval of overturning and bouncing movements made by the cutting robot. The stability condition is not met at the probability of 39 %; hence, cutting fails to proceed smoothly, leading to an accident.

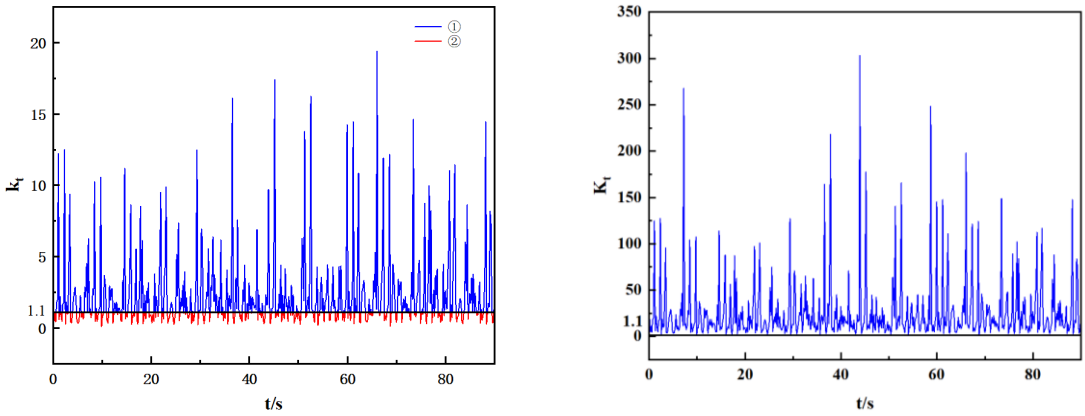

Figure 8: Change curves of the cutting-induced bouncing stability coefficient; a) Stability without bracing, b) Stability with bracing.

The changes in the stability coefficient k_t when the support force of the oil cylinders (4 ones) for the upper and lower shields of the temporary support robot was taken as F_{2y} (4F) > 5865 KN are displayed in Fig. 9. The stability coefficient was constantly greater than 1.1, which could ensure the smooth implementation of cutting.

Vibration displacement response of the cutting robot: On the basis of the previously established multirigid-body dynamic model, the robot's cutting drum, cutting arm, sliding table, upper shield, and lower shield were subjected to longitudinal and transverse random displacement response simulation analyses. The simulation time was set to 90 s, being the cutting time for one section, the cutting speed to 2.3 m/min, and the drum speed to 25 r/min.

The random displacement response and the transverse random displacement response of the cutting drum, cutting arm, sliding table, lower shield, and upper shield during the downward (longitudinal) cutting process are exhibited in Fig. 9.

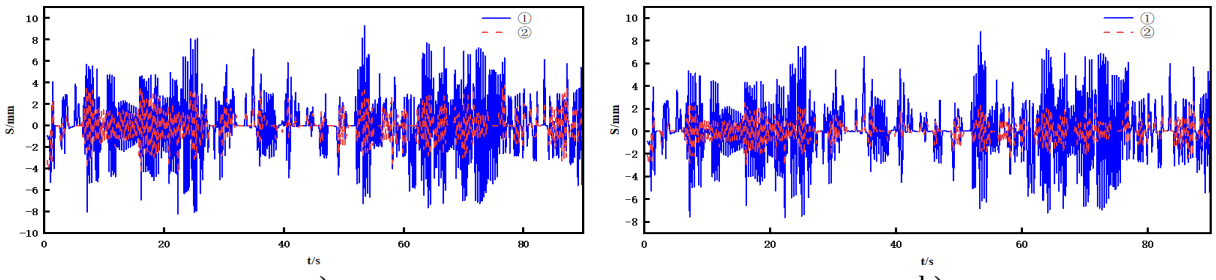

Figure 9: Displacement response of each part of the robot; a) The cutting drum, b) The cutting arm.

In Fig. 9, ① indicates the longitudinal displacement, and ② represents the transverse displacement. According to the displacement response diagram and Table I, in the sectional cutting process, the maximum, minimum, and mean values of the longitudinal random responses of the cutting drum, cutting arm, sliding table, and upper and lower shields were all greater than the transverse displacements. The maximum, minimum, and mean values of the displacements from the cutting drum to the upper and lower shields gradually decreased, and

the displacements of the upper and lower shields were almost negligible. Because the picks on the cutting drum were symmetrically arranged on both sides, the transverse vibration displacement was effectively reduced. In addition, the upper and lower shields of the shield structure supported the roof and floor of the cut roadway, effectively playing a stabilizing role in the cutting process, reducing the system displacement, controlling the vibration of each component of the robot, ensuring the smooth cutting process, and guaranteeing the cutting quality.

Table I: Displacement response of the cutting drum, cutting arm, sliding table and upper and lower shields.

Robot component	**Value feature**	**Longitudinal displacement** /mm	**Transverse displacement** /mm
Cutting drum	Maximum value	9.27	3.77
	Minimum value	−8.23	−4.50
Cutting arm	Maximum value	8.78	2.69
	Minimum value	−7.65	−3.06
Sliding table	Maximum value	3.24	0.51
	Minimum value	−3.33	−0.53
Lower shield	Maximum value	1.94	0.31
	Minimum value	−2.00	−0.32
Upper shield	Maximum value	1.62	0.26
	Minimum value	−1.67	−0.26

4.2 Test analysis

Based on the established mechanical model and simulation experiment of the shield-type tunnelling robot and the actual situation of the Xiaobaodang mine roadway, a field test was designed to test the vibration and displacement response of the cutting drum, cutting arm, sliding table, and upper and lower shields. The test platform is a shield-type rapid tunnelling system. High-precision displacement sensors were installed on the cutting drum, the sliding table, the cutting arm, and the contact surface between the upper and lower shields and the roof and floor of the roadway, as shown in Fig. 10.

Figure 10: Rapid tunnelling system and laser displacement sensors.

One section, which was 4250 mm in height and 4400 mm in width, was cut in the field roadway test at a cutting depth of 300 mm, a cutting speed of 2.3 m/min, and a drum speed of 25 r/min.

The shield lifting cylinder could output a thrust of 1530 KN. From the above analysis, when $F \geq 5865$ KN, the stability condition was met and the thrust of each lifting cylinder was greater than 1466 KN. In the test, the thrust of a single lifting cylinder was 1500 KN. The effect of the cross-section cutting test is shown in Fig. 11.

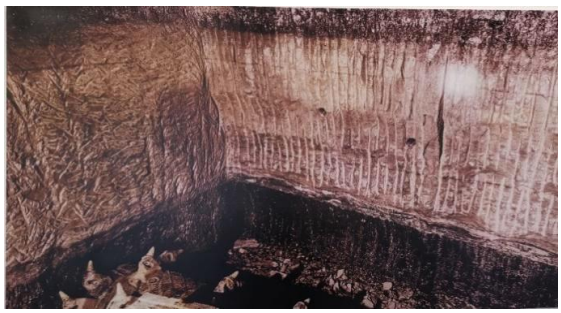

Figure 11: Sectional cutting effect after the shield supports the lifting cylinder and pressurization is implemented.

On the premise of meeting cutting conditions, the displacement response of the cutting drum, is displayed in Fig. 12.

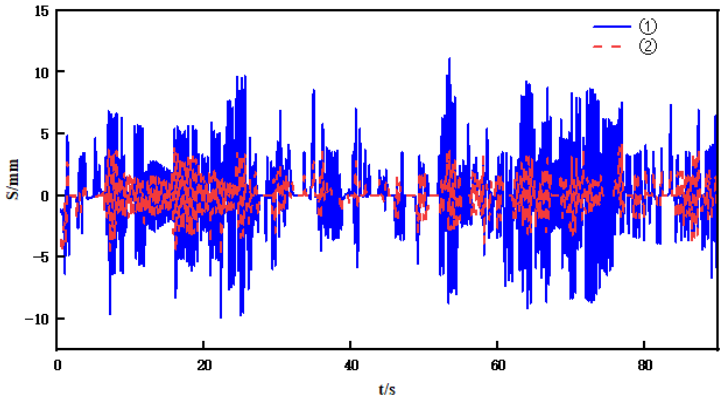

Figure 12: Displacement response of the cutting drum.

From Fig. 12 that the longitudinal displacement responses of the cutting drum, the cutting arm, the sliding table and the upper and lower shields were all greater than the transverse displacement responses, the displacement responses decreased in turn, and the closer to the cut section, the greater the displacement response. The transverse displacement responses were evidently smaller than the longitudinal displacements because the cutting robot performed drum-type cutting, and the cutting picks were symmetrically installed on the cutting drum, which could largely keep the cutting forces on both sides of the drum balanced, resulting in minor vibration. The vibration displacement responses declined in turn for two reasons: First, the cutting drum was connected to the section, serving as the source of vibration. Second, the shield-type structure could support the roadway roof and floor, significantly reducing the vibration of the cutting system and enhancing the system stability.

Comparison of the simulation and test results of each component's displacement response indicated that the tested displacement response should be generally greater than the simulated value, and the relative error between the test and simulation values was 6 %–26 %. The reason is as follows: The roadway operation field conditions were complicated, and the vibration was great because of the influences of the roadway size and shape, sectional partition, and the friction of the cutting robot system.

5. CONCLUSION

This study assessed the stability of a shield-type tunnelling robot and the vibration displacement response law of the system components to improve the tunnelling-cutting stability and reduce the impact of vibration on the system. The following conclusions were acquired through simulation and test:

(1) A load model for the cutting drum of the shield-type tunnelling robot was established, and the relationships of cutting parameters with the cutting resistance and tractive resistance borne in the cutting process were determined.

(2) The stability coefficient for the shield-type tunnelling robot system was proposed. A pressure of 5865 KN, when a shield-supported cylinder was used to cut coal and rock with hardness of f6, was determined to be the condition for keeping the system stable.

(3) Through simulation and test methods, the vibration displacement responses of the cutting drum, cutting arm, sliding table, and upper and lower shields were found to be increasingly smaller, and the maximum transverse and longitudinal displacements were 9.27 and 11.68 mm, respectively.

This study is of great significance for improving the large-sectional semi-coal and rock cutting stability of coal mines and reducing the vibration displacement response. In the follow-up study, an intelligent perception method will be integrated so that the system can perceive the vibration of each component to some extent, which will help further relieve the influence of vibration on the cutting process and improve the system stability and cutting efficiency.

REFERENCES

[1] Wang, G.; Zhao, G.; Ren, H. (2019). Analysis on key technologies of intelligent coal mine and intelligent mining, *Journal of China Coal Society*, Vol. 44, No. 1, 34-41, doi:10.13225/j.cnki.jccs.2018.5034

[2] Wang, G. (2022). New technological progress of coal mine intelligence and its problems, *Coal Science and Technology*, Vol. 50, No. 1, 1-27, doi:10.13199/j.cnki.cst.2022.01.011

[3] Ma, Z. (2020). Current situation and development trend of the integrated equipment of digging and anchoring, *Colliery Mechanical & Electrical Technology*, Vol. 41, No. 5, 11-13, doi:10.16545/j.cnki.cmet.2020.05.003

[4] Miao, W.; Yan, S.; Li, J. (2020). Development status and trend of excavation equipment with bolting unit at home and abroad, *Journal of Machine Design*, Vol. 37, No. S1, 287-290, doi:10.13841/j.cnki.jxsj.2020.s1.074

[5] Acaroglu, O.; Ergin, H. (2006). A new method to evaluate roadheader operational stability, *Tunnelling and Underground Space Technology*, Vol. 21, No. 2, 172-179, doi:10.1016/j.tust.2005.04.004

[6] Dogruoz, C.; Bolukbasi, N. (2014). Effect of cutting tool blunting on the performances of various mechanical excavators used in low-and medium-strength rocks, *Bulletin of Engineering Geology and the Environment*, Vol. 73, No. 3, 781-789, doi:10.1007/s10064-013-0551-y

[7] Dewangan, S.; Chattopadhyaya, S. (2016). Performance analysis of two different conical picks used in linear cutting operation of coal, *Arabian Journal for Science & Engineering*, Vol. 41, No. 1, 249-265, doi:10.1007/s13369-015-1786-7

[8] Choi, S.-O.; Lee, S.-J. (2015). Three-dimensional numerical analysis of the rock-cutting behavior of a disc cutter using particle flow code, *KSCE Journal of Civil Engineering*, Vol. 19, No. 4, 1129-1138, doi:10.1007/s12205-013-0622-4

[9] Anderson, K. S.; Duan, S. (2000). Highly parallelizable low-order dynamics simulation algorithm for multi-rigid-body systems, *Journal of Guidance, Control and Dynamics*, Vol. 23, No. 2, 355-364, doi:10.2514/2.4531

[10] Goktan, R. M.; Gunes, N. (2005). A comparative study of Schmidt hammer testing procedures with reference to rock cutting machine performance prediction, *International Journal of Rock Mechanics and Mining Sciences*, Vol. 42, No. 3, 466-472, doi:10.1016/j.ijrmms.2004.12.002

[11] Ergin, H.; Acaroglu, O. (2007). The effect of machine design parameters on the stability of a roadheader, *Tunneling and Underground Space Technology*, Vol. 22, No. 1, 80-89, doi:10.1016/j.tust.2006.04.003

[12] Yuan, X.; Zou, Y.; Zong, X.; Peng, Y.; Zhang, L. (2017). Research on cutting performance of cutting header on part-face roadheader, *Journal of Mechanical Engineering*, Vol. 53, No. 24, 193-200, doi:10.3901/jme.2017.24.193

[13] Wang, D.; Huang, J.; Zheng, W.; Jiang, W.; Yang, C. (2023). Sensitive relationship between cutting load and cutting state parameters of boom-type roadheader, *Coal Engineering*, Vol. 55, No. 5,123-129
[14] Hu, M.; Zhang, X.; Han, K. (2021). Dynamic characteristics analysis and optimization of roadheader cutting head, *Coal Technology*, Vol. 40, No. 11, 217-219, doi:10.13301/j.cnki.ct.2021.11.053
[15] Wang, P.; Zong, K.; Zhang, B.; Chen, S.; Cheng, L. (2018). Boom-type roadheader cutting process analysis of body's position and attitude change based on ADAMS simulation, *Coal Technology*, Vol. 37, No. 6, 250-252, doi:10.13301/j.cnki.ct.2018.06.094
[16] Cha, T. (2021). Analysis of static stability of driving and anchoring integrated machine, *Coal Mine Machinery*, Vol. 42, No. 5, 71-73, doi:10.13436/j.mkjx.202105023
[17] Li, Z.-C. (2006). Analysis of operational stability of roadheader, *Coal Mine Machinery*, Vol. 2006, No. 4, 590-592
[18] Wang, P. (2009). Study on stability for transverse-cutting of cantilevered roadheader, *Coal Mine Machinery*, Vol. 30, No. 5, 64-66, doi:10.13436/j.mkjx.2009.05.049
[19] Huang, L. (2018). Analysis and study on working stability of half coal rock roadheader, *Coal Technology*, Vol. 37, No. 9, 288-291, doi:10.13301/j.cnki.ct.2018.09.106
[20] Hu, F.; Wei, X.; Xu, P.; Bai, Y. (2022). Analysis of longitudinal stability under extreme working condition of EBZ260 roadheader, *Coal Mine Machinery*, Vol. 43, No. 1, 81-82, doi:10.13436/j.mkjx.202201024
[21] Wang, X. (2011). Static stability analysis of EBH315 roadheader, *Coal Mine Machinery*, Vol. 32, No. 12, 102-103, doi:10.13426/j.mkjx.2011.12.099
[22] Ladu, J. L. C.; Lu, X.-W. (2014). Effects of hydraulic retention time, temperature, and effluent recycling on efficiency of anaerobic filter in treating rival domestic wastewater, *Water Science and Engineering*, Vol. 7, No. 2, 168-182, doi:10.3882/j.issn.1674-2370.2014.02.005
[23] De Klerk, D.; Ossipov, A. (2010). Operational transfer path analysis: Theory guidelines and tire noise application, *Mechanical Systems and Signal Processing*, Vol. 24, No. 7, 1950-1962, doi:10.1016/j.ymssp.2010.05.009
[24] Xie, M.; Shi, J.; Zhang, H.; Zhu, Y. (2023). Prediction of longitudinal vibration characteristics of new vertical-axis roadheader under multiple excitation, *Chinese Journal of Engineering Design*, Vol. 30, No. 6, 728-737
[25] Kovacic, B.; Mursec, L.; Lubej, S. (2022). Synchronisation of contactless vibration monitoring methods, *International Journal of Simulation Modelling*, Vol. 21, No. 1, 113-123, doi:10.2507/IJSIMM21-1-594
[26] Mao, J.; Song, B.-X.; Yao, L.; Sun, Z. (2011). The dynamics characteristics research and simulation for cutting components of roadheader, *Microcomputer Information*, Vol. 27, No. 4, 16-17
[27] Li, X.; He, Y.; Li, T.; Yang, T. (2014). Analysis of transverse and longitudinal random vibration response of longitudinal axis roadheader, *Journal of China Coal Society*, Vol. 39, No. 3, 580-585, doi:10.13225/j.cnki.jccs.2013.0370
[28] Ma, H.; Wang, P.; Zhang, X.; Cao, X.; Mai, Q. (2020). Research on key technology of intelligent tunneling robotic system in coal mine, *Joumal of Xi'an University of Science and Technology*, Vol. 40, No. 5, 751-759, doi:10.13800/j.cnki.xakjdxxb.2020.0501
[29] Dong, L.; Zhang, H.; Lu, J.; Shi, R. (2022). Rock cutting characteristics with single pick and prediction of cutting force based on force chain, *Rock and Soil Mechanics*, Vol. 43, No. 11, 3036-3046, doi:10.16285/j.rsm.2022.5008
[30] Wei, R.; Jin, H. (2020). Dynamic stability analysis software design of tunneling machine based on VB and Matlab, *Journal of Mechanical Strength*, Vol. 42, No. 3, 631-638, doi:10.16579/j.issn.1001.9669.2020.03.018
[31] Fox, B.; Jennings, L. S.; Zomaya, A. Y. (1999). Numerical computation of differential-algebraic equations for nonlinear dynamics of multibody systems involving contact forces, *Journal of Mechanical Design*, Vol. 123, No. 2, 272-281, doi:10.1115/1.1353587